Targeted Therapy Resistance Mediated by Dynamic Regulation of Extrachromosomal Mutant EGFR DNA

David A. Nathanson *et al.*

Science **343**, 72 (2014);
DOI: 10.1126/science.1241328

21. B. T. Lahn, D. C. Page, *Science* **278**, 675–680 (1997).
22. S. E. Kleiman *et al.*, *Hum. Reprod.* **22**, 151–158 (2007).
23. Practice Committee of American Society for Reproductive Medicine, *Fertil. Steril.* **90** (suppl.), S199–S201 (2008).
24. L. Gianaroli *et al.*, *Fertil. Steril.* **72**, 539–541 (1999).
25. A. Saremi, N. Esfandiari, N. Salehi, M. R. Saremi, *Arch. Androl.* **48**, 315–319 (2002).
26. K. L. Tamashiro, Y. Kimura, R. J. Blanchard, D. C. Blanchard, R. Yanagimachi, *J. Assist. Reprod. Genet.* **16**, 315–324 (1999).
27. J. A. Graves, *Cell* **124**, 901–914 (2006).
28. J. F. Hughes *et al.*, *Nature* **463**, 536–539 (2010).
29. J. M. Riel *et al.*, *J. Cell Sci.* **126**, 803–813 (2013).
30. Y. Yamauchi, J. M. Riel, Z. Stoytcheva, P. S. Burgoyne, M. A. Ward, *Genome Biol.* **11**, R66 (2010).

Acknowledgments: The work was supported by NIH HD072380, HD058059, and GM103457 (Project 2) and Hawaii Community Foundation 13ADVC-60314 grants to M.A.W. The authors thank P. Burgoyne for providing paternal stock mice for breeding, overall support, and insightful discussions and N. Vernet from P. Burgoyne's group for sharing protocols and expertise on histological and DNA content analyses. We are grateful to numerous students who have helped with mouse genotyping. Histological sections were prepared by John A. Burns School of Medicine Histopathology Core supported by NIH grants National Institute on Minority Health and Health Disparities, NIH. G12 MD007601 and the National Institute of General Medical Sciences, NIH, P30 GM103341.

Supplementary Materials
www.sciencemag.org/content/343/6166/69/suppl/DC1
Materials and Methods
Supplementary Text
Figs. S1 to S8
Table S1
References (*31*–*50*)

28 June 2013; accepted 28 October 2013
Published online 21 November 2013;
10.1126/science.1242544

Targeted Therapy Resistance Mediated by Dynamic Regulation of Extrachromosomal Mutant EGFR DNA

David A. Nathanson,[2] Beatrice Gini,[1]* Jack Mottahedeh,[5]* Koppany Visnyei,[5] Tomoyuki Koga,[1] German Gomez,[1] Ascia Eskin,[10] Kiwook Hwang,[3,4] Jun Wang,[3,4] Kenta Masui,[1] Andres Paucar,[2,5] Huijun Yang,[1] Minori Ohashi,[2] Shaojun Zhu,[1] Jill Wykosky,[1] Rachel Reed,[1] Stanley F. Nelson,[10] Timothy F. Cloughesy,[7,8] C. David James,[6] P. Nagesh Rao,[9] Harley I. Kornblum,[2,5,7]† James R. Heath,[3,4]† Webster K. Cavenee,[1,11]† Frank B. Furnari,[1,11]† Paul S. Mischel[1,11]†‡

Intratumoral heterogeneity contributes to cancer drug resistance, but the underlying mechanisms are not understood. Single-cell analyses of patient-derived models and clinical samples from glioblastoma patients treated with epidermal growth factor receptor (EGFR) tyrosine kinase inhibitors (TKIs) demonstrate that tumor cells reversibly up-regulate or suppress mutant EGFR expression, conferring distinct cellular phenotypes to reach an optimal equilibrium for growth. Resistance to EGFR TKIs is shown to occur by elimination of mutant *EGFR* from extrachromosomal DNA. After drug withdrawal, reemergence of clonal *EGFR* mutations on extrachromosomal DNA follows. These results indicate a highly specific, dynamic, and adaptive route by which cancers can evade therapies that target oncogenes maintained on extrachromosomal DNA.

The majority of targeted therapies have not produced substantial survival benefits for most cancer patients (*1*, *2*). A variety of resistance mechanisms have been described, including incomplete target suppression, second-site mutations, and activation of alternative kinases to maintain signal flux to downstream effector pathways (*1*–*3*). Thus, most efforts are now aimed at developing better drugs or better drug combinations to more fully suppress the target oncogenes and their downstream signals. Changes in the cellular composition of tumors, particularly in response to targeted treatment, could facilitate such a resistance mechanism and thereby dictate patient response.

In glioblastoma (GBM), the most common malignant primary brain cancer of adults, the epidermal growth factor receptor (*EGFR*) is frequently mutated, commonly giving rise to the constitutively active oncogenic variant *EGFRvIII* (*4*, *5*). EGFRvIII potently accelerates tumor growth by cell-autonomous and intercellular signaling mechanisms (*6*), but it also makes tumor cells that express it more sensitive to EGFR tyrosine kinase inhibitors (TKIs) (*7*, *8*). In clinical GBM samples, the level of EGFRvIII protein expression varies widely among cells within the tumor mass (*6*, *9*–*15*). The potential contribution of heterogeneous EGFRvIII expression to EGFR TKI resistance in GBM (*16*) is not understood.

To determine whether EGFRvIII heterogeneity contributes to EGFR TKI resistance, single-cell analyses of a patient-derived EGFRvIII-expressing xenograft model (GBM39) (*17*) were performed. GBM39 cells stably express firefly luciferase (ff-LUC), enabling definitive tumor cell identification (fig. S1A). Quantitative microfluidic image cytometry (MIC) (*18*) demonstrated detectable levels of EGFRvIII protein in 60% (±5%) of tumor cells (fig. S1B). The EGFRvIII-expressing tumor cells ($EGFRvIII^{High}$) demonstrated increased phosphatidylinositol 3-kinase–Akt–mammalian target of rapamycin (PI3K-Akt-mTOR) signaling (Fig. 1A and fig. S2), elevation in tumor cell proliferation by a factor of 4 (Fig. 1B and fig. S2), a lower basal apoptotic rate by a factor of 15 (Fig. 1C and fig. S2), and increased glucose uptake (Fig. 1D) relative to the GBM cells lacking detectable EGFRvIII protein ($EGFRvIII^{Low}$) (Fig. 1, D and E). Further, the $EGFRvIII^{High}$ tumor cells showed enhanced cell death in response to the EGFR TKI erlotinib (Fig. 1F).

To determine the effect of an EGFR TKI on EGFRvIII population dynamics, mice bearing tumors were treated daily with oral erlotinib (150 mg per kg of weight). Erlotinib treatment initially caused 80% tumor shrinkage (response) (blue line in Fig. 1G), shifting the composition of tumors from being predominantly $EGFRvIII^{High}$ to predominantly $EGFRvIII^{Low}$ tumor cells (Fig. 1H and fig. S3). This shift in the EGFRvIII population dynamics was maintained, even after tumors developed resistance to continued erlotinib treatment (resistant) [Fig. 1G (red line) and H, and fig. S3], and was also detected in another patient-derived ex vivo neurosphere culture, HK296 (fig. S4). Most important, in tumor tissue from GBM patients treated for 7 to 10 days with the EGFR/HER2 inhibitor lapatinib, the relative fraction of $EGFRvIII^{High}$ tumor cells dramatically declined relative to each patient's pretreatment sample (Fig. 1, I and J). Of note, this analysis was confined to patients whose posttreatment tumor tissue showed reduced EGFR phosphorylation relative to the pretreatment sample. We did not detect any decrease in EGFRvIII level in the two available GBMs in which no decrease in phospho-EGFR was seen after lapatinib treatment.

[1]Ludwig Institute for Cancer Research, University of California at San Diego, La Jolla, CA, USA. [2]Department of Molecular and Medical Pharmacology, David Geffen UCLA School of Medicine, Los Angeles, CA 90095, USA. [3]NanoSystems Biology Cancer Center, California Institute of Technology, Pasadena, CA, USA. [4]Division of Chemistry and Chemical Engineering, California Institute of Technology, MC 127-72, Pasadena, CA 91030, USA. [5]Neuropsychiatric Institute–Semel Institute for Neuroscience and Human Behavior and Department of Psychiatry and Biobehavioral Sciences, David Geffen UCLA School of Medicine, Los Angeles, CA 90095, USA. [6]University of California San Francisco, San Francisco, CA 94143, USA. [7]Henry Singleton Brain Tumor Program and Jonsson Comprehensive Cancer Center, David Geffen UCLA School of Medicine, Los Angeles, CA 90095, USA. [8]Department of Neurology, David Geffen UCLA School of Medicine, Los Angeles, CA 90095, USA. [9]Department of Pathology and Laboratory Medicine, David Geffen UCLA School of Medicine, Los Angeles, CA 90095, USA. [10]Department of Human Genetics, David Geffen UCLA School of Medicine, Los Angeles, CA 90095, USA. [11]UCSD School of Medicine, La Jolla, CA 92093, USA.

*These authors contributed equally to this work.
†This work is based on equal contributions from the laboratories of H.I.K, J.R.H, W.K.C, F.B.F, and P.S.M
‡Corresponding author. E-mail: pmischel@ucsd.edu

Unexpectedly, EGFRvIII^{High}/EGFRvIII^{Low} GBM subpopulations sorted by fluorescence-activated cell sorting (FACS) proved to be equally tumorigenic, giving rise to heterogeneous tumors (Fig. 2, A and B). Seeds containing ~200, 2000, or 20,000 cells of FACS-sorted EGFRvIII^{High}/EGFRvIII^{Low} subpopulations generated subcutaneous tumors of similar size, containing the same ratio of EGFRvIII^{High}/EGFRvIII^{Low} cells as the original tumor (Fig. 2C). FACs-sorted pure populations of EGFRvIII^{High} and EGFRvIII^{Low} GBM cells plated at 2 to 5 cells per well, or even as single cells per well, gave rise to colonies containing a similar ratio of EGFRvIII^{High}/EGFRvIII^{Low} cells (Fig. 2, D to F). These findings are consistent with a stochastic state transition model, in which distinct tumor subpopulations regenerate the phenotypic equilibrium characteristic of the original tumor (*19*). Erlotinib treatment completely suppressed this state transition and maintained the population in an EGFRvIII^{Low} state, and it continued to do so long after any tumor cell death was observed (fig. S5).

To determine the mechanism by which GBM cells modulate EGFRvIII protein levels during erlotinib resistance, we generated a reversible EGFR TKI resistance model by continuous treatment of GBM cells with erlotinib in GBM39 cells in neurosphere culture, followed by drug withdrawal (Fig. 3, A to C), and examined the level, sequence, and subnuclear localization of *EGFRvIII* DNA. EGFRvIII arises from an in-frame genomic deletion of exons 2 to 7 of the EGFR gene and has been thought to reside primarily on small circular extrachromosomal fragments of DNA called double-minute (DM) chromosomes (*20*–*22*). Fluorescent in situ hybridization (FISH) of naïve (n = 15 metaphases), erlotinib-resistant (n = 15 metaphases), and drug-removed (n = 10 metaphases) GBM39 metaphase cells with EGFR and centromere 7–specific DNA probes revealed abundant *EGFR*$^+$ extrachromosomal DNA in naïve and drug-removed tumor cells and a complete loss of these *EGFR*$^+$ extrachromosomal DNA elements in erlotinib-resistant GBM cells (Fig. 3D). No changes in chromosomal *EGFR* copy number were detected between naïve, erlotinib-resistant, or drug-removed GBM cells. The overall FISH signal patterns were confirmed by analysis of more than 100 interphase nuclei from each of the three conditions (fig. S7). The loss of *EGFR*$^+$ extrachromosomal DNA in erlotinib resistance was specific, because these cells still contained abundant extrachromosomal DNA elements (fig. S6), including *MDM2*$^+$ DMs, which were identified by FISH and polymerase chain reaction (PCR)–Southern blot analysis. The *MDM2*$^+$ DM copy number rose with erlotinib treatment and remained elevated, even after drug withdrawal (fig. S8). In each erlotinib-resistant metaphase or interphase cell, a single

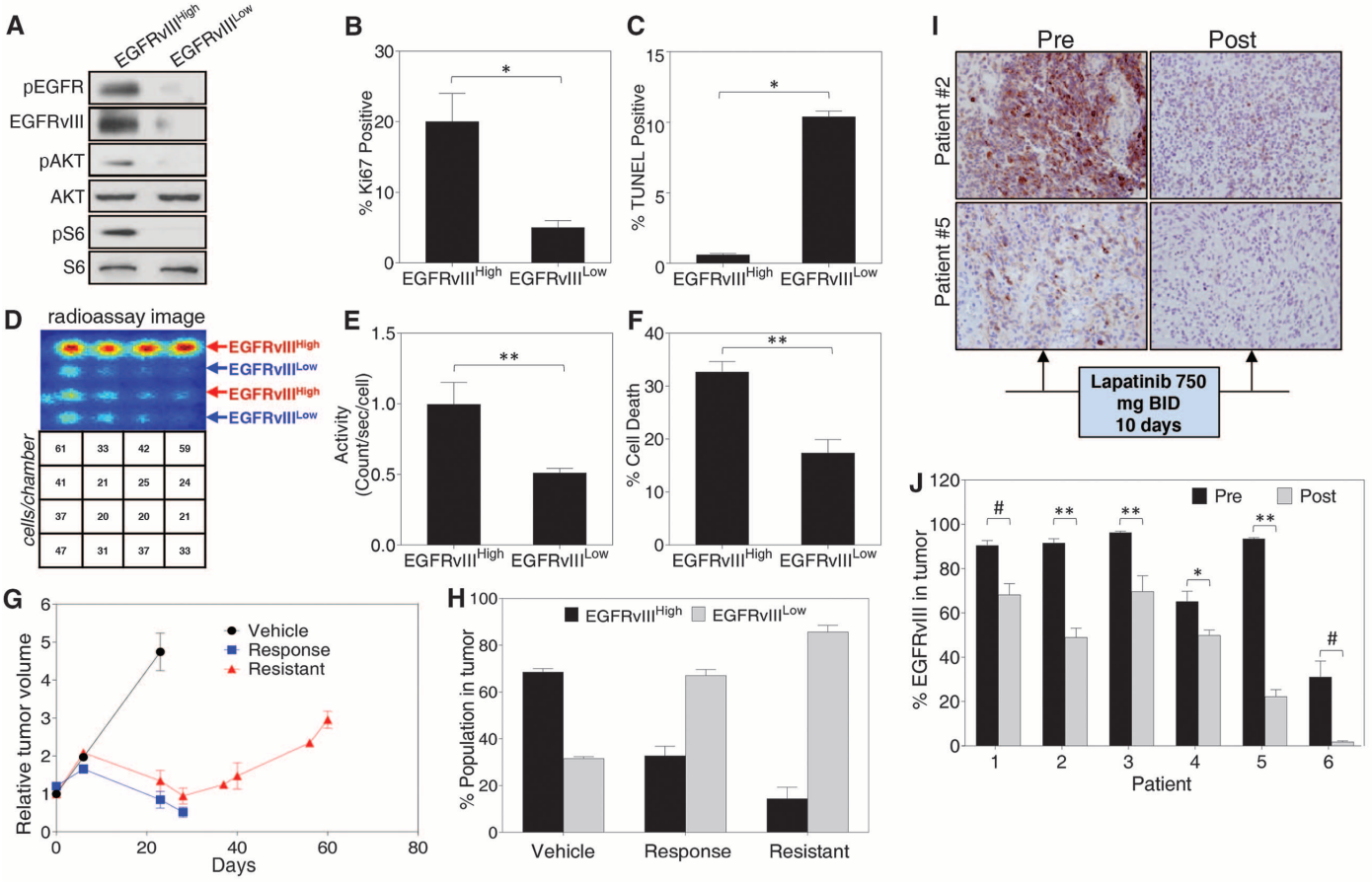

Fig. 1. Resistance to EGFR TKIs in preclinical models and GBM patients treated with an EGFR TKI is associated with a decreasing ratio of EGFRvIII^{High}/EGFRvIII^{Low} tumor cells. (**A**) FACS-sorted EGFRvIII^{High} and EGFRvIII^{Low} cells obtained from GBM39 differ in their PI3K-Akt-mTOR activity as determined by immunoblotting. (**B**) Immunofluorescence (IF) for EGFRvIII and K_i-67 on isolated GBM39 tumor cells shows differences in basal proliferative rate between EGFRvIII^{High} and EGFRvIII^{Low} tumor cells. *P < 0.005. (**C**) Terminal deoxynucleotidyl transferase–mediated deoxyuridine triphosphate nick end labeling (TUNEL) stain and EGFRvIII IF indicate a higher basal apoptosis in EGFRvIII^{Low} tumor cells. *P < 0.005. (**D** and **E**) Radiopharmaceutical imaging chip analysis of ^{18}F-fluorodeoxyglucose from FACS-sorted EGFRvIII^{High} and EGFRvIII^{Low} cells indicates higher glucose uptake in EGFRvIII^{High} cells. **P < 0.05. (**F**) FACS-sorted EGFRvIII^{High} and EGFRvIII^{Low} were treated with erlotinib (5 μM) for 24 hours, and cell viability was determined by trypan blue exclusion assay. **P < 0.05. (**G** and **H**) Resistance to erlotinib in GBM39 xenografts (n = 4 mice per group). During initial response (blue curve) and at the time of resistance (red curve), there is a relative loss of EGFRvIII-expressing tumor cells. (**I** and **J**) In GBM patients, 10 days of treatment with the EGFR tyrosine kinase inhibitor lapatinib reduces EGFRvIII expression relative to pretreatment levels. *P < 0.01; **P < 0.0001; #P < 0.001. All values are mean ± SEM. P values were obtained from unpaired t test.

marker chromosome made up of homogeneous staining regions (HSRs) positive for *EGFR*, but lacking the chromosome 7–specific centromere sequences, was detected. Similar HSR-like *EGFR*$^{+}$ marker chromosomes were detected in naïve and drug-removed GBM metaphases, raising the possibility that these bodies may serve as a latent reservoir for EGFRvIII in erlotinib-resistant GBM cells (Fig. 3D and fig. S9).

To confirm that the *EGFR*$^{+}$ extrachromosomal elements were *EGFRvIII*, we performed Southern blot, PCR, and sequencing analyses of low-molecular-weight extrachromosomal DNA (Fig. 3, E to I). A 4.1-kb band in BamH1-digested low-molecular-weight DNA indicative of *EGFRvIII* was detected in naïve and drug-removed GBM39 cells but not erlotinib-resistant cells (Fig. 3, E and F). The intronic breakpoints that give rise to the *EGFRvIII* deletion are not consistent, varying between individuals (*23*). Therefore, we designed primers mapping at each of the 17 BamH1 restriction sites spanning the region of interest. PCR and Southern blot analyses identified a genomic deletion confirmed to be EGFRvIII by sequencing of cloned fragments (fig. S10 and Fig. 3, E to I). We identified the intronic breakpoints giving rise to *EGFRvIII* in two additional patient-derived GBM ex vivo neurosphere cultures (GBM6 and HK296) (fig. S10) (*24*, *25*) and measured extrachromosomal *EGFRvIII* DNA copy number in naïve and erlotinib-resistant cells, including after drug withdrawal, by a quantitative PCR assay. Consistent with the effect of erlotinib in GBM39 cells, continuous EGFR TKI treatment caused almost complete loss of extrachromosomal *EGFRvIII* DNA and erlotinib resistance (Fig. 4A and fig. S11). Remarkably, cessation of erlotinib treatment for as little as 72 hours in GBM6 and HK296 markedly increased extrachromosomal *EGFRvIII* DNA and resensitized tumor cells to erlotinib-induced cell death (fig. S11).

The availability of two pairs of matched formalin-fixed, paraffin-embedded tissue sections from patients pre- and post-lapatinib treatment (patients 2 and 3 from Fig. 1, I and J) enabled us to perform FISH using probes for EGFR (which recognizes EGFRvIII) and centromere 7. In both patients, a nearly 80% reduction in EGFR FISH-positive signals after lapatinib treatment was detected (Fig. 4B), thus indicating the clinical relevance of loss of extrachromosomal EGFRvIII DNA as an EGFR TKI resistance mechanism. In this cohort of patients, intratumoral lapatinib levels sufficient to cause tumor cell death (2000 to 3000 nM) were not achieved in the tumor samples (*7*). However, 1500 nM of lapatinib, an intratumoral level observed in at least some of these patients, was sufficient to cause highly significant reduction of extrachromosomal EGFRvIII DNA in GBM39, GBM6, and HK296 neurospheres in culture (fig. S12), suggesting that the significant reduction seen in patients 2 and 3 was a consequence of lapatinib treatment.

Analysis of an additional four matched sets of EGFRvIII-positive tumor tissue from GBM patients before and after treatment with conventional therapy (temozolomide and radiation) showed no detectable difference in extrachromosomal EGFR FISH-positive DNA levels (Fig. 4C). Taken together, these results indicate that loss of extrachromosomal *EGFRvIII* DNA is a general and clinically relevant EGFR TKI resistance mechanism in GBM.

It is unusual for EGFRvIII to be homogeneously expressed in a tumor, despite the selective growth advantage conferred to individual GBM cells (Fig. 1, B, C, E, and F). EGFRvIII possibly imposes a cost to tumor cells, potentially by increasing nutrient requirements (Fig. 1D). Notably, the EGFR TKI resistance mechanism identified here is entirely distinct from the mechanism by which GBMs maintain EGFRvIII heterogeneity in the absence of treatment. Extrachromosomal *EGFRvIII* DNA copy number remains elevated in the treatment-naïve EGFRvIII^{Low} cells (fig. S13), consistent with an epigenetic regulatory mechanism of EGFRvIII heterogeneity (*15*). Taken together, these results highlight the exquisite specificity of reversible loss of extrachromosomal *EGFRvIII* DNA as a GBM EGFR TKI resistance mechanism.

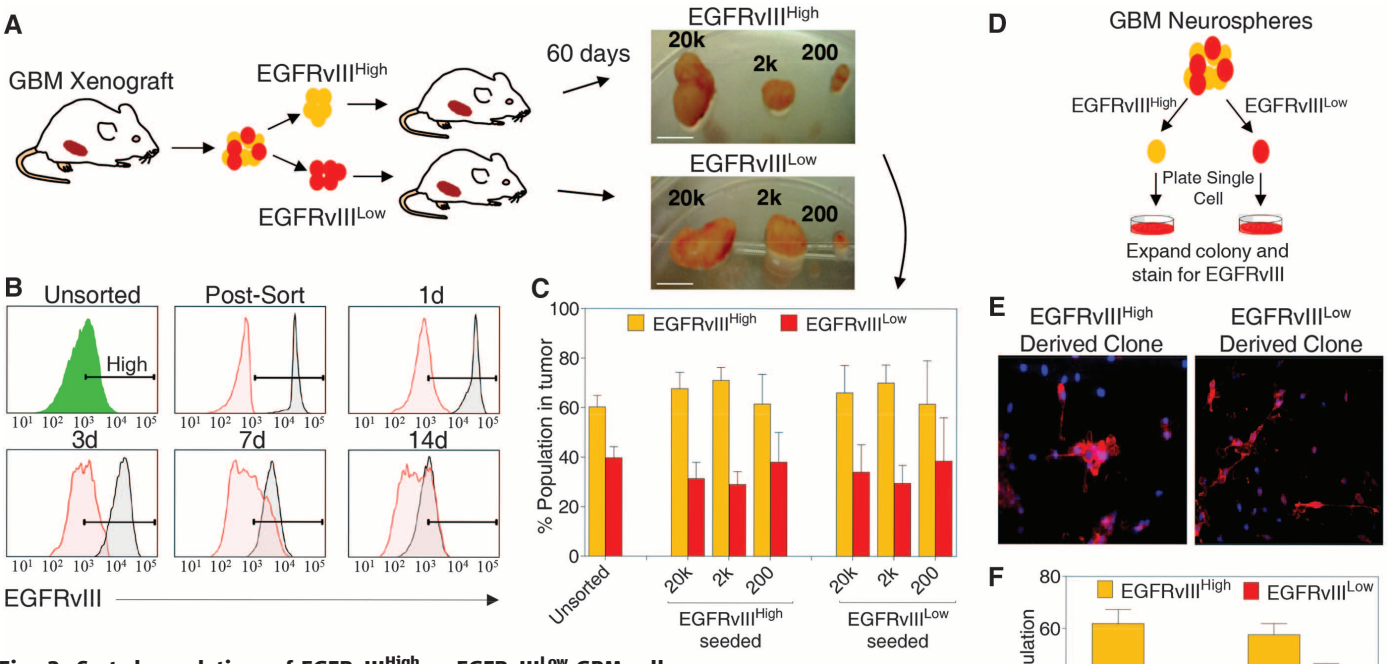

Fig. 2. Sorted populations of EGFRvIII^{High} or EGFRvIII^{Low} GBM cells give rise to identical mixed tumors in vivo. (**A**) Tumor cells from GBM39 xenografts sorted for EGFRvIII expression and injected into mice are equally tumorigenic (n = 4 mice per group). The white line indicates 1 inch. (**B**) FACS analysis of sorted cells reveals that enriched populations of EGFRvIII^{High} and EGFRvIII^{Low} tumor cells re-establish mixed populations within 2 weeks. (**C**) Analysis of xenograft models deriving from sorted EGFRvIII^{High} and EGFRvIII^{Low} tumor cell populations from (A) that give rise to tumors with an EGFRvIII^{High}/EGFRvIII^{Low} tumor cell composition similar to that of initial, untreated GBM39 tumors. Values are mean ± SEM. (**D** and **E**) GBM39 tumor cells sorted for EGFRvIII expression and plated at a single cell per well and stained for EGFRvIII (red) and 4′,6-diamidino-2-phenylindole (DAPI) (blue) give rise to heterogeneous colonies. (**F**) Identical EGFRvIII^{High}/EGFRvIII^{Low} composition from tumor cells sorted in (D) and plated at 2 to 5 cells per well. Values are mean ± SEM from n = 5 independent cultures.

EGFRvIII^{High} GBMs display enhanced apoptotic sensitivity to EGFR TKIs (Fig. 1F). However, our data suggest that EGFR TKI resistance may not be mediated entirely by selection for a subpopulation of tumor cells lacking extrachromosomal *EGFRvIII* DNA but may also involve rapid single-step elimination, as has been described for loss of the *DHFR* gene on double minutes in the absence of methotrexate (*26*, *27*) and the loss of *MYCC* or *MYCN* from double minutes in the presence of hydroxyurea (*28*). These independent and complementary mechanisms of EGFRvIII regulation, coupled to intercellular signaling between EGFRvIII^{High}/EGFRvIII^{Low} tumor cells (*6*), enable GBMs to achieve an EGFRvIII^{High}/EGFRvIII^{Low} ratio that is optimal for growth and survival, including in response to EGFR TKI therapy. Future work is needed to examine the compensatory mechanisms that enable GBM cells lacking *EGFRvIII* extrachromosomal DNA to continue to proliferate during EGFR TKI treatment, including the potential role of extrachromosomal *MDM2* amplification, and possible changes along the spectrum of epithelial mesenchymal transition, including irreversible up-regulation of ZEB-1 (fig. S14), which recently has been shown to promote plasticity and tumorigenicty of breast cancer cells (*29*).

Resistance to targeted therapies is a nearly universal clinical challenge for cancer patients (*1*, *3*). Daily dosing with the EGFR TKIs is not optimal because it is hard to achieve sufficient levels of intratumoral EGFR inhibition (*7*). Pulsatile intermittent treatment with much higher doses of an EGFR TKI could potentially lead to better target inhibition and even possibly less toxicity relative to continuous dosing. In other cancers, a "drug holiday" can resensitize tumors to targeted therapy (*30*). The data presented here provide a conceptual mechanistic rationale for pulsatile intermittent EGFR TKI dosing in GBM to achieve better target inhibition while permitting tumors to regain drug sensitivity as extrachromosomal *EGFRvIII* DNA levels rapidly rise between treatments (fig. S11). These results provide an unexpected twist showing that loss of *EGFRvIII* extrachromosomal DNA promotes resistance, in contrast to the current paradigm of drug resistance through increased levels of extrachromosomal

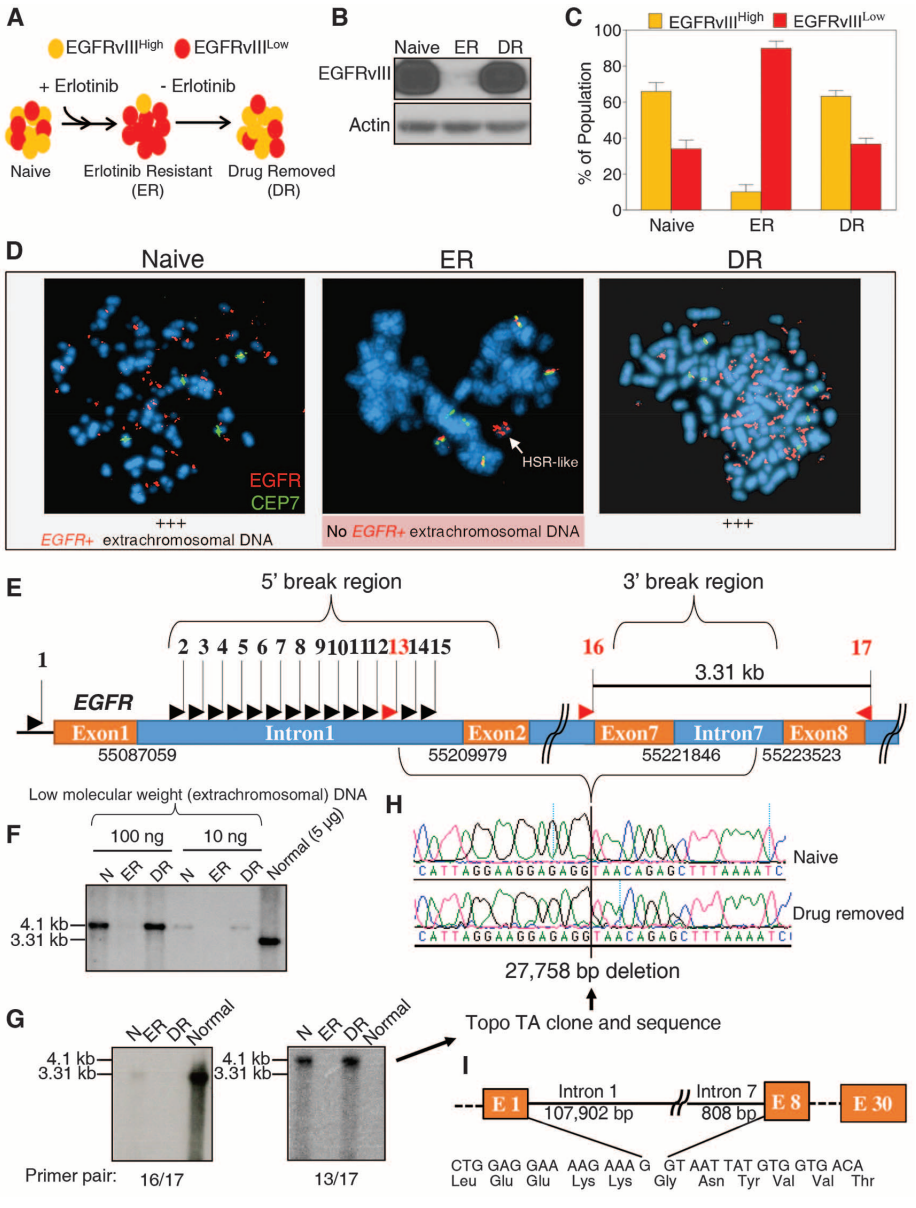

Fig. 3. GBM cells suppress EGFRvIII protein expression on prolonged exposure to erlotinib and up-regulate it upon drug withdrawal by restoring EGFR^{+} extrachromosomal DNA elements. (**A**) Schematic model of reversible EGFR TKI resistance model. GBM39 cells were maintained in neurosphere culture and were treated continuously with vehicle (naïve) or erlotinib [5 μM, erlotinib-resistant (ER), 60 days]. Drug was removed from the ER neurospheres for 30 days [drug-removed (DR)]. (**B**) Immunoblot of EGFRvIII levels for naïve, ER, and DR cells. (**C**) MIC chip quantification of the ratio of EGFRvIII^{High} and EGFRvIII^{Low} tumor cells in naïve, ER, and DR cells. (**D**). DAPI-stained metaphases of naïve, ER, and DR cells probed with *EGFR* (red) and chromosome 7 centromere probes (CEP7, green) with abundant *EGFR*$^{+}$ extrachromosomal DNA elements in naïve and DR GBM cells. No extrachromosomal *EGFR*$^{+}$ DNA elements were detected in any of the ER metaphase spreads. The white arrow shows *EGFR*$^{+}$ HSR-like staining of a marker chromosome lacking centromere 7. One such DNA element was found in metaphases from each ER GBM cell analyzed. They were also detected in some naïve and drug-removed metaphases. (**E**) Map of EGFR gene between exon 1 and intron 8. (**F**) Southern blot analysis shows binding of EGFR probe (red line) to low-molecular-weight DNA, which is lost during resistance and reemerges with drug withdrawal. Normal genomic DNA is used as control for EGFR probe. (**G**) PCR using primers spanning each of the 17 Bam H1 restriction sites from 5′ of exon 1 through intron 8 (see supplementary materials) was used to identify EGFRvIII or wild-type EGFR. Primer pairs 13/17 and 14/17 span regions that are 32 kb apart in wild-type EGFR but only slightly more than 4 kb in EGFRvIII. Primer pairs 13/17 and 14/17 cannot amplify wild-type EGFR but result in amplification of EGFRvIII from low-molecular-weight DNA of naïve and drug-removed GBM39 cells. No EGFRvIII was detected in erlotinib-resistant GBM39 cells. Primers 15 and 16 are both deleted in EGFRvIII but maintained in wild-type EGFR. Primer pair 16/17 yields a 3.3-kb wild-type EGFR band in normal control DNA. Representative images of primer pairs 16/17 and 13/17 are shown. (**H** and **I**) Sequencing of the cloned fragments reveals identical intronic breakpoints associated with a 27,785–base pair deletion of exon 3 to 7 sequences and resulting in EGFRvIII transcript and protein in treatment-naïve and drug-removed GBM39 cells.

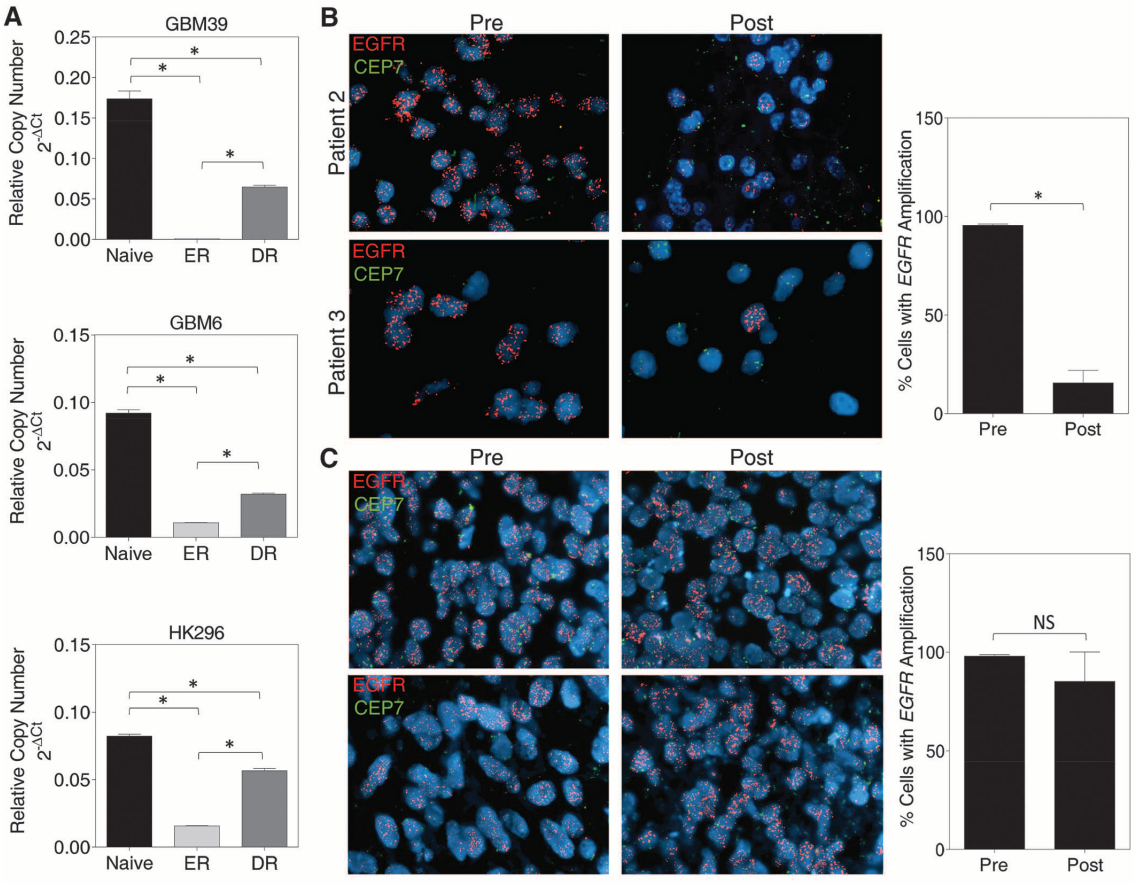

Fig. 4. Loss of *EGFR* extrachromosomal DNA elements in GBM patient samples treated with EGFR TKI. (**A**) Quantitative PCR analysis of EGFRvIII extrachromosomal DNA in three GBM patient-derived neurosphere lines. Erlotinib resistance for GBM6 and HK296 was established by continuous erlotinib treatment (1 μM) for 30 days. DR for GBM6 and HK296 was established after removing erlotinib from ER cultures for 3 days. Conditions for GBM39 were described above. Values are mean ± SEM from $n > 9$ replicates. *$P < 0.0001$ from unpaired *t* test. (**B**) Representative images (left) and quantification (right) from dual-color FISH (CEP7, green; EGFR, red) performed on pre/post matched pairs of GBM tissue sections from $n = 2$ patients treated with lapatinib for 10 days (patients #2 and #3 from Fig. 1J). Nuclei were counterstained with DAPI. Values are mean ± SD. *$P < 0.005$ from unpaired *t* test. (**C**) Representative images (left) and quantification (right) from dual-color FISH (CEP7, green; EGFR, red) performed on pre/post matched pairs of GBM tissue sections from $n = 4$ EGFRvIII-positive patients treated with radiation and concomitant chemotherapy using standard dosing of temozolomide. Nuclei were counterstained with DAPI. Values are mean ± SD.

DNA carrying drug resistance genes (*31*, *32*). These results also highlight the diversity of mechanisms by which extrachromosomal DNA can promote resistance to targeted cancer therapies. A number of other oncogenes have been identified on extrachromosomal DNA (*33*), potentially enabling them to respond rapidly to targeted drug treatment (*34*). It is possible that resistance in other tumor types in which the main oncogene is extrachromosomal may be similarly mediated by loss of the oncogene on extrachromosomal DNA.

References and Notes

1. B. Vogelstein *et al.*, *Science* **339**, 1546–1558 (2013).
2. L. A. Garraway, P. A. Jänne, *Cancer Discov.* **2**, 214–226 (2012).
3. M. S. Glickman, C. L. Sawyers, *Cell* **148**, 1089–1098 (2012).
4. R. Bonavia, M. M. Inda, W. K. Cavenee, F. B. Furnari, *Cancer Res.* **71**, 4055–4060 (2011).
5. C. W. Brennan *et al.*, *Cell* **155**, 462–477 (2013).
6. M. M. Inda *et al.*, *Genes Dev.* **24**, 1731–1745 (2010).
7. I. Vivanco *et al.*, *Cancer Discov* **2**, 458–471 (2012).
8. I. K. Mellinghoff *et al.*, *N. Engl. J. Med.* **353**, 2012–2024 (2005).
9. P. A. Humphrey *et al.*, *Proc. Natl. Acad. Sci. U.S.A.* **87**, 4207–4211 (1990).
10. S. N. Kurpad *et al.*, *Glia* **15**, 244–256 (1995).
11. K. D. Aldape *et al.*, *J. Neuropathol. Exp. Neurol.* **63**, 700–707 (2004).
12. R. Nishikawa *et al.*, *Brain Tumor Pathol.* **21**, 53–56 (2004).
13. A. B. Heimberger *et al.*, *Clin. Cancer Res.* **11**, 1462–1466 (2005).
14. J. Jeuken *et al.*, *Brain Pathol.* **19**, 661–671 (2009).
15. C. A. Del Vecchio *et al.*, *Oncogene* **32**, 2670–2681 (2013).
16. A. A. Brandes, E. Franceschi, A. Tosoni, M. E. Hegi, R. Stupp, *Clin. Cancer Res.* **14**, 957–960 (2008).
17. C. Giannini *et al.*, *Neuro-oncol.* **7**, 164–176 (2005).
18. J. Sun *et al.*, *Cancer Res.* **70**, 6128–6138 (2010).
19. P. B. Gupta *et al.*, *Cell* **146**, 633–644 (2011).
20. S. H. Bigner *et al.*, *Cancer Res.* **50**, 8017–8022 (1990).
21. N. Vogt *et al.*, *Proc. Natl. Acad. Sci. U.S.A.* **101**, 11368–11373 (2004).
22. J. Z. Sanborn *et al.*, *Cancer Res.* **73**, 6036–6045 (2013).
23. L. Frederick, X. Y. Wang, G. Eley, C. D. James, *Cancer Res.* **60**, 1383–1387 (2000).
24. J. N. Sarkaria *et al.*, *Mol. Cancer Ther.* **6**, 1167–1174 (2007).
25. H. D. Hemmati *et al.*, *Proc. Natl. Acad. Sci. U.S.A.* **100**, 15178–15183 (2003).
26. D. A. Haber, R. T. Schimke, *Cell* **26**, 355–362 (1981).
27. R. J. Kaufman, P. C. Brown, R. T. Schimke, *Mol. Cell. Biol.* **1**, 1084–1093 (1981).
28. D. D. Von Hoff *et al.*, *Proc. Natl. Acad. Sci. U.S.A.* **89**, 8165–8169 (1992).
29. C. L. Chaffer *et al.*, *Cell* **154**, 61–74 (2013).
30. M. Das Thakur *et al.*, *Nature* **494**, 251–255 (2013).
31. D. Ercan *et al.*, *Oncogene* **29**, 2346–2356 (2010).
32. R. T. Schimke, R. J. Kaufman, F. W. Alt, R. F. Kellems, *Science* **202**, 1051–1055 (1978).
33. S. E. Benner, G. M. Wahl, D. D. Von Hoff, *Anticancer Drugs* **2**, 11–26 (1991).
34. N. Shimizu, *Cytogenet. Genome Res.* **124**, 312–326 (2009).

Acknowledgments: This work was supported by the Ben and Catherine Ivy Foundation Fund (P.S.M., J.R.H., and T.F.C.); by National Institutes of Health (NIH) grants NS73831 (P.S.M.), U54 CA151819 (P.S.M. and J.R.H., principal investigator), P01-CA95616 (W.K.C. and F.B.F.), R01-NS080939 (F.B.F.), and NINDS R01 NS052563 (H.I.K.); and by the Ziering Family Foundation in memory of Sigi Ziering (T.F.C. and P.S.M.), the Art of the Brain Fund (T.F.C.), the James S. McDonnell Foundation (to F.B.F.), the European Commission PIOF-GA-2010-271819 (B.G.), Ruth L. Kirschstein Institutional National Research Service Award T32 CA009056 (D.A.N.), and the UCLA Scholars in Oncologic Molecular Imaging (SOMI) Program (D.A.N.). W.K.C. is a Fellow of the National Foundation for Cancer Research. We thank R. Kolodner for careful reading of the manuscript and helpful suggestions. We also thank W. Yong and the UCLA Brain Tumor Translational Resource.

Supplementary Materials

www.sciencemag.org/content/343/6166/72/suppl/DC1
Materials and Methods
Figs. S1 to S14
References

3 June 2013; accepted 14 November 2013
Published online 5 December 2013;
10.1126/science.1241328